

Received July 2, 2021, accepted July 13, 2021, date of publication July 26, 2021, date of current version August 9, 2021.

Digital Object Identifier 10.1109/ACCESS.2021.3100506

# Finite-Set Model Predictive Current Control of Induction Motors by Direct Use of Total Disturbance

MAHDI S. MOUSAVI<sup>1</sup>, S. ALIREZA DAVARI<sup>1</sup>, (Senior Member, IEEE), VAHAB NEKOUKAR<sup>1</sup>, CRISTIAN GARCIA<sup>2</sup>, (Member, IEEE), AND JOSE RODRIGUEZ<sup>3</sup>, (Life Fellow, IEEE)

<sup>1</sup>Department of Electrical Engineering, Shahid Rajaei Teacher Training University, Tehran 1678815811, Iran

<sup>2</sup>Department of Electrical Engineering, Universidad de Talca, Curico 3340000, Chile

<sup>3</sup>Faculty of Engineering, Universidad Andres Bello, Santiago 7550196, Chile

Corresponding author: S. Alireza Davari (davari@sru.ac.ir)

The work of Cristian Garcia and Jose Rodriguez was supported by the Agencia Nacional de Investigación y Desarrollo (ANID) through the Project under Grant FB0008 and Grant ACT192013, and in part by the Fondo Nacional de Desarrollo Científico y Tecnológico (FONDECYT) under Grant 1210208 and Grant 11180235.

**ABSTRACT** Disturbance rejection strategies are very useful for the robustness improvement of the predictive control method. But they can only be used in the modulated-based predictive control methods such as continuous set model predictive control (CS-MPC) and deadbeat control. This paper presents a robust current prediction model based on total disturbance observer (TDO), which is applicable in the finite set model predictive current control (FS-MPCC). In the proposed method, the disturbance is directly used as a part of the prediction model instead of the disturbance rejection loop. So, the proposed method has two advantages over the disturbance rejection-based CS-MPC schemes. The first advantage is no need for a controller, which is an essential part of the disturbance rejection-based CS-MPC. Therefore, the proposed method is simpler and has fewer control parameters. The second feature is that the proposed model is in the stationary frame. In this way, the frame transformation is avoided in the prediction model. Moreover, to guarantee zero steady-state error in the current prediction model, this paper proposes a complete designing process for TDO based on the convergence analysis. The performance of the proposed control system is evaluated through simulations and experimental tests.

**INDEX TERMS** Induction motor drive, robust predictive control, PCC, FS-MPCC, disturbance rejection.

## I. INTRODUCTION

Model predictive control (MPC) theory has been extensively studied in power electronics over the past decade [1]. The idea of MPC is based on applying the system model to predict the future behavior of the variable states [2]. In regards to the prediction process, successful methods can be categorized into two major groups. In the first group, the system variables are continuously predicted, and a pulse width modulation (PWM) technique is used to generate the switching states of the power converter. This strategy is known as the continuous set model predictive control (CS-MPC) [3]. The other group is the so-called finite set model predictive control (FS-MPC). In FS-MPC, the future state of the controlled variables is predicted based on the possible voltage vectors (VV) of the power converter. Among these predicted states, the VV of the

state that minimizes the predefined cost function is selected, and it is applied to the power converter [4].

In the field of induction motor (IM) drives, the MPC method has been widely used with different strategies. Predictive current control (PCC) is one of the common MPC strategies that can be applied in both deadbeat, and FS-MPC approaches [5], [6]. This method does not require a weighting factor in the cost function. The performance of PCC schemes particularly depends on the current prediction model. Since the conventional model of IM contains some uncertainties such as parameter mismatch and unmodeled dynamics, several papers have tried to improve the robustness of PCC [6]–[9]. A modified prediction model has been presented in [7] and a current prediction model with closed-loop sliding mode control has been proposed in [9] to improve the robustness of MPC against the parametric uncertainty. Using adaptive control theory is another method for robustness improvement of MPC. Model reference adaptive

The associate editor coordinating the review of this manuscript and approving it for publication was Mauro Gaggero<sup>1</sup>.

system (MRAS) has been frequently implemented in MPC schemes to observe the accurate value of a sensitive variable or estimate an uncertain parameter of the plant [3], [10], [11].

Recently, the disturbance observer-based technique (DOB) has been studied for the robustness improvement of the MPC with two purposes: compensation of the uncertain load torque and compensation of the uncertain model of the motor. There are comprehensive studies in the first category [6], [9], [12] in which the goal is the robustness of the speed control loop. The focus of this paper is on the second purpose, which is the enhancement of the prediction model. In this way, DOB techniques have been utilized to eliminate the effect of parameter mismatch in the prediction model of the deadbeat PCC scheme [8]. While the parameter variation has been reflected in this strategy, the prediction model is still based on the conventional model of IM. This model contains several uncertain variables that can affect prediction accuracy. To overcome this problem, some recent studies have tried to replace the conventional prediction model. For this purpose, novel control theories have been used, e.g., auto disturbance rejection control (ADRC) [13]–[15], model-free control (MFC) [15], [16], and recursive least square (RLS) techniques [17], [18].

ADRC is a control method that only utilizes the input and the output of a plant without using its parameters [19]. The main idea of ADRC is based on considering the “total disturbance”, i.e., all of the disturbances and model uncertainties as an extended state variable of the system, which is extracted by using an extended state observer (ESO). In this manner, the coupling between the state variables, system unmodeled dynamics, external disturbances, and other similar uncertainties can be easily managed in the control scheme [19]. Due to this outstanding feature, ADRC has been applied to the various control systems, including IM drive [20]–[23]. Lately, ADRC has been implemented in the speed control loop of MPC [14]. But the classic prediction model has been used in this method.

In MFC theory, the derivatives of the system output are directly expressed by the input using an ultra-local model [24]. In this theory, an unknown variable presents all the unknown dynamics, unknown parts, and possible disturbances of the system, and it must be estimated with online identification techniques. Model-free predictive control (MFPC) has been proposed based on the MFC theory to enhance the robustness of predictive control methods [15], [16]. However, the identification of the unknown variable of the ultra-local model needs a complex mathematical process. For a first-order system, the ultra-local model in MFC is the same as the system model in ADRC. Considering this concept, an MFPC has been proposed in [15] without the complex identification process. This method employs a linear ESO from ADRC theory to estimate the unknown variables of MFPC.

Although the replacement of the conventional model of a plant with an ultra-local model in MFPC or with the model of ADRC theory significantly improves the robustness

of a predictive control method, this strategy is suitable for CS-MPC or deadbeat control methods, and it's not normally applicable in FS-MPC schemes. Because in ADRC and similarly in MFPC [15], the observed unknown variable must be subtracted from the control law to generate the suitable voltage references of the inverter. While in FS-MPC, the control law is replaced by the cost function, which selects the suitable voltage vector of the inverter. FS-MPC can be a parameter-free method by employing the RLS techniques in the current prediction model [17], [18]. In this scheme, the next-step stator current is recursively predicted by using the past current samples. So, the prediction model does not require the motor parameters, and it is robust against their variations. In [17], despite the robust performance of the RLS-based MPC, the need for saving enough information about the previous samples increases the processing time of this method. In [18], the model of the plant is updated in each sampling time by using a real-time data-driven RLS technique, which does not require high computation burden.

This paper manipulates the total disturbance concept in ADRC to solve the problem of the lack of compatibility with FS-MPC methods. To achieve this goal, the total disturbance is directly used in the prediction model instead of a subtraction term from the control law. Therefore, a novel current prediction model is proposed in this paper, which directly uses the outputs of TDO. Unlike the MFPC and ADRC based MPC, the proposed method is implemented with FS-MPC. There are two differences between the implementation of disturbance observer in the proposed FS-MPC and CS-MPC methods. The first difference is that the proposed method does not require a controller for the disturbance rejection loop because it manipulates the total disturbance in a feed-forward formation and, a cost function is utilized for controlling the stator current. While in CS-MPC, after regulating the stator current in the controller, the observed disturbance is compensated as feedback [25]. Therefore, the proposed method is simpler and has fewer control parameters. The second difference is that, unlike the disturbance rejection method in CS-MPC, the proposed TDO based prediction model is applied in the stationary frame. Hence, the frame transformation is omitted, which removes the uncertainty of the rotor position from the prediction model.

In the proposed method, the model of the plant is updated in real-time by using TDO. Therefore, all of the IM dynamics and un-measured conditions like the core loss are considered in the proposed model. The proposed TDO estimates an unknown function which is the representation of those modeled and unmodeled dynamics. So, the parameters of IM and the variables like fluxes and rotor speed have not appeared in the current prediction model. Besides the robustness improvement of the proposed TDO, the number of the TDO parameters is fewer than that of the IM, and they are not time-variant. Moreover, this paper proposes a complete designing process for TDO based on the convergence analysis.

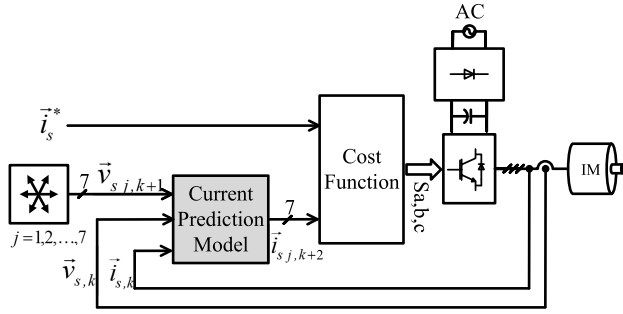


FIGURE 1. General block diagram of the FS-MPCC.

## II. PRINCIPLE OF FINITE SET MODEL PREDICTIVE CURRENT CONTROL (FS-MPCC)

This method is based on predicting the future currents of the motor for the finite number of the switching states. If a two-level voltage source inverter is used, the number of candidates will be seven. The best switching state is selected by means of a cost function. Fig. 1 shows the block diagram of the FS-MPCC method.

This technique consists of three main parts:

- 1) **Inputs:** the stator currents are measured by the sensors and the current references are calculated by an outer control loop. The outer control loop is not investigated in this research and it is chosen as a classical linear controller.
- 2) **The current prediction model:** the current prediction for seven states is performed by this model. Totally, seven future current vectors are predicted by the prediction model. So, it plays a key role in the MPC.
- 3) **The cost function:** the error between the reference and predicted currents is used for switching state selection. Each cost function is related to a switching state. The state that minimizes the cost function will be selected. The following equation is the cost function of the predictive current control.

$$G_j = \left| \vec{i}_s^* - \vec{i}_{s,jk+2} \right|_{j=1, \dots, 7} \quad (1)$$

where  $\vec{i}_s^*$  represents the reference vector of the stator current. The real and imaginary components of this vector are respectively obtained by the flux reference and the speed controller [26]. Note that the flux reference can be set as constant or it can be attained by the field weakening methods. Also,  $\vec{i}_{s,jk+2}$  is the predicted stator current vector related to the  $j$ th switching state.

## III. CLASSIC DISTURBANCE REJECTION BASED PREDICTIVE CURRENT CONTROL

The concept of ‘‘total disturbance’’ was firstly introduced by Han in [19] to control the uncertain systems with the disturbance rejection methods. In this idea, only the input and the output of the system are utilized to derive the control law, without knowing other parts of the system, which may be nonlinear, time-varying, or uncertain. This extra part is

considered as a system state, and it is estimated by a state observer in real-time. By using this technique, the disturbances and uncertainties in many systems can be overcome. The application of this method to the predictive method is mostly based on the deadbeat principle. The dynamic equation of the motor is used to calculate the voltage reference.

$$\vec{i}_{s,k+1} = \vec{i}_{s,k} + t_s \left( -\frac{1}{\sigma \tau_s} - \frac{1}{\sigma \tau_r} + j\omega_r \right) \vec{i}_{s,k} + \frac{t_s}{\sigma L_s} \left( \frac{1}{\tau_r} - j\omega_r \right) \vec{\lambda}_{s,k} + \frac{t_s}{\sigma L_s} \vec{v}_s \quad (2)$$

where  $\tau_s = L_s/R_s$ ,  $\tau_r = L_r/R_r$ , and  $\sigma = 1 - L_m^2/L_s L_r$ . Also,  $\vec{v}_s$  represents the stator voltage,  $\vec{i}_s$  is the stator current, and  $\vec{\lambda}_s$  denotes the stator flux.  $R_s$  and  $R_r$  are the stator and rotor resistances, respectively.  $L_s$ ,  $L_r$  and  $L_m$  respectively are the stator, rotor, and mutual inductances.  $\omega_r$  is the electrical speed, and  $t_s$  is the sampling time.

The calculated voltage reference is compensated by the observed distortion ( $\hat{d}$ ) [27], [28].

$$\vec{v}_s^* = \left( \frac{\sigma L_s}{t_s} \right) \left( \vec{i}_{s,k+1}^* - \vec{i}_{s,k} \right) - \sigma L_s \left( -\frac{1}{\sigma \tau_s} - \frac{1}{\sigma \tau_r} + j\omega_r \right) \vec{i}_{s,k} - \left( \frac{1}{\tau_r} - j\omega_r \right) \vec{\lambda}_{s,k} - \hat{d} \quad (3)$$

where  $\vec{i}_{s,k+1}^*$  is the current reference, and  $\vec{v}_s^*$  is the calculated voltage reference. Finally, the calculated voltage reference is applied to the motor by the PWM technique.

Application of this method in the FS-MPCC is not possible because the voltage reference calculation is eliminated from this method, and it is replaced by a cost function based direct switching method. Furthermore, the dependency of (3) to the classic parameters of the motor is still high. These gaps are addressed in this research.

## IV. PROPOSED CURRENT PREDICTION MODEL

### A. COMPATIBILITY WITH THE FINITE SET CONCEPT

The disturbance rejection is used in the other way round by the proposed method to develop a technique compatible with FS-MPC. Firstly, the stator current difference equation is written as below by means of disturbance theory.

$$\vec{i}_{s,k+1} = \vec{i}_{s,k} + t_s \left( \hat{D}_k + b \vec{v}_{s,k} \right) \quad (4)$$

where  $b$  is the input coefficient, which is selected by a rough approximation of the input coefficient in (2).  $\hat{D}$  represents the total disturbance, which is covering all of the uncertainties, disturbances, and unmodeled dynamics of IM, which is estimated by TDO in the real-time process.

Now considering  $\hat{D}_k$  as the estimation of the total disturbance, the current prediction for all feasible VVs of the inverter is performed by the disturbance based model (5).

$$\vec{i}_{s,1, \dots, 7, k+1} = \vec{i}_{s,k} + t_s \left( \hat{D}_k + b \vec{v}_{s,0, \dots, 7} \right) \quad (5)$$

$$\vec{v}_{s,1, \dots, 7} = \frac{2}{3} V_{dc} \left( s_a + s_b a + s_c a^2 \right) \quad (6)$$

where  $V_{dc}$  is the voltage of the inverter's DC-link,  $a = e^{j2\pi/3}$  and  $s_a, s_b,$  and  $s_c$  denote the switching states of the inverter. Each of these switching states can take two possible values, i.e., 1 or 0.

It must be noted that the proposed method manipulates the ADRC theory to achieve a prediction model for the FS-MPC strategy. To this end, The proposed method directly uses the total disturbance in the model, while ADRC cancels that in the control law by feedback. Moreover, the proposed method is utilized as an FS-MPC scheme by changing the structure of ADRC to a feed-forward prediction model, which does not require the controller of the ADRC method. The proposed method can also be applied in the other MPC techniques, which contain a current prediction model. Hence, this method can be used in the model predictive torque control.

**B. TOTAL DISTURBANCE OBSERVER**

The proposed prediction model (4) cannot be used without the estimation of the total disturbance ( $\hat{D}$ ). In the ADRC theory, the total disturbance is considered as the state of the plant. Therefore, it can be estimated by designing an observer, which is called total disturbance observer (TDO) [19]. For system (4), the stator current is the state. So, the error of the current i.e.,  $e = \hat{i}_{s,k-1} - i_{s,k-1}$  is used for disturbance observation as follows.

$$\begin{cases} \hat{i}_{s,k} = \hat{i}_{s,k-1} + t_s(\hat{D}_{k-1} + b\vec{v}_{s,k-1} + \beta_1 e) \\ \hat{D}_k = \hat{D}_{k-1} + t_s\beta_2 f(e) \end{cases} \quad (7)$$

where superscript “^” shows the estimated values and  $f(e)$  is a nonlinear function defined as follows [19]

$$f(e) = \begin{cases} \sqrt{|e|} \cdot \text{sgn}(e), & |e| > \delta \\ e/\sqrt{\delta}, & |e| \leq \delta \end{cases} \quad (8)$$

where the performance of the observer with the function “ $f(e)$ ” is in between the sliding mode observer and Luenberger observer [29]. In the sliding mode observer, the amount of the error is not considered in the feedback. On the other hand, in Luenberger observer, the error is linearly injected into the model. So, the big errors which are resulted from the measuring noise and are not real errors reduce the accuracy of the observer. It is clear that the utilized nonlinear function is saturated when the error is increasing. Also,  $\beta_1$  and  $\beta_2$  are the feedback gains of the observer. Totally, there are three parameters for the TDO, i.e.,  $\delta, \beta_1,$  and  $\beta_2$ .

The complete block diagram of the proposed current prediction model is depicted in Fig. 2. The disturbance is used to predict the stator current for the possible solutions. Therefore, opposite to the normal disturbance rejection methods, the disturbance is the base of the prediction in the proposed method. For the practical implementation, the delay compensation must be performed for the predicting algorithm. In the proposed TDO, the next sampling intervals of the stator current  $\hat{i}_{s,k+1}$  and the disturbance  $\hat{D}_{k+1}$  can be obtained by

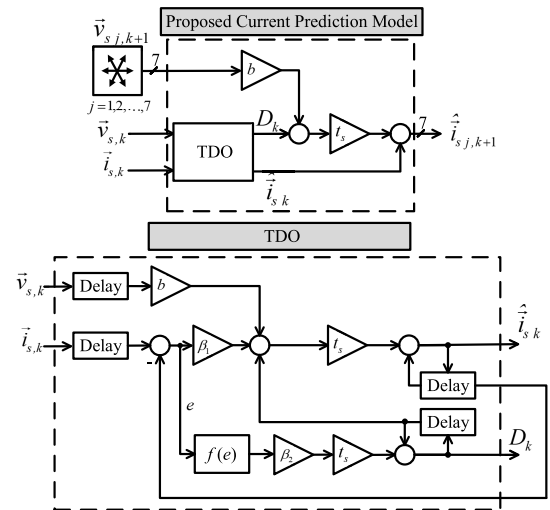


FIGURE 2. Proposed current prediction model.

putting the current state of the variables in (7). By using the outputs of TDO in (5), the predicted stator current  $\hat{i}_{s,j,k+2}$  is achieved for the feasible VVs.

**V. TUNING TDO PARAMETERS**

Though the parameters of the proposed model are mostly independent of the motor parameters there is not a thorough guideline for tuning them. An analytical guideline is proposed in this research based on the stability analysis of TDO. The stability analysis is completely discussed by applying Lyapunov theory in the appendix. Note that the equations for both orthogonal components are similar and the designed parameters are valid for both.

**A. PARAMETERS “ $\beta_1$ ” AND “ $\beta_2$ ”**

The most important part of the TDO design is selecting proper values for  $\beta_1$  and  $\beta_2$ . The convergence analysis which is presented in the appendix results in the following criterion.

$$\frac{1}{4\sqrt{\delta}}\beta_1^2 > \beta_2 > M \quad (9)$$

where  $M$  is the maximum value of the disturbance's derivative, i.e.,  $M = \max(dD/dt)$ . To find a rough approximation of  $M$ , (2) and the following approximations are used:

$$\begin{aligned} \max\left(\frac{d^2|i_s|}{dt^2}\right) &= \max\left(\frac{d}{dt}\left[\left(-\frac{1}{\sigma\tau_s} - \frac{1}{\sigma\tau_r} + j\omega_r\right)|i_s\right.\right. \\ &\quad \left.\left.+ b\left(\frac{1}{\tau_r} - j\omega_r\right)|\lambda_s| + b|v_s|\right]\right) \\ &\simeq \max\left(\omega_r\frac{d|i_s|}{dt} - b\omega_r\frac{d|\lambda_s|}{dt} + b\frac{d|v_s|}{dt}\right) \end{aligned} \quad (10)$$

Note that its assumed that  $\omega_{rn} > 10\frac{1}{\tau_s}$  and  $\omega_{rn} > 10\frac{1}{\tau_r}$  which is a rational assumption. Then, by considering  $\max(dy/dt) = 2\pi f_n y_n$ , where  $y$  is an arbitrary variable,  $f_n$  is the nominal frequency, and  $y_n$  is the nominal magnitude of  $y$ ,



(10) can be simplified as below:

$$\max\left(\frac{d^2|i_s|}{dt^2}\right) \simeq 2\pi f_n (\omega_{r_n} i_{s_n} - b\omega_{r_n} \lambda_{s_n} + b v_{s_n}) \quad (11)$$

$M$  can be calculated by using (4) and (11) as below:

$$M = 2\pi f_n \omega_{r_n} (i_{s_n} - b\lambda_{s_n}) \quad (12)$$

where  $f_n$  is the nominal frequency,  $\omega_{r_n}$  is rated speed,  $i_{s_n}$  denotes the nominal stator current, and  $\lambda_{s_n}$  is the nominal flux. As shown in (12),  $M$  is related to the nominal values of IM. Note that, the nominal values of a motor are general information without any uncertainties. As mentioned, there is no need for accurate calculation of  $M$ . It is a rough approximation of  $\max(dD/dt)$  because based on (9), it is enough to select parameter  $\beta_2$  large enough. In [19],  $\beta_1^2 = 3\beta_2$  is suggested to satisfy (9). Therefore, the following equations are suitable to tune the gains of the feedback in TDO.

$$\beta_1 = 2\sqrt{M}, \quad \beta_2 = \frac{4}{3}M \quad (13)$$

### B. PARAMETER “b”

If the error of the input coefficient ( $\Delta b$ ) is considered as a part of the total disturbance  $\vec{D}$ , the following equation is achieved.

$$\frac{d\vec{i}_s}{dt} = \vec{D} + \Delta b \vec{v}_s + b \vec{v}_s \quad (14)$$

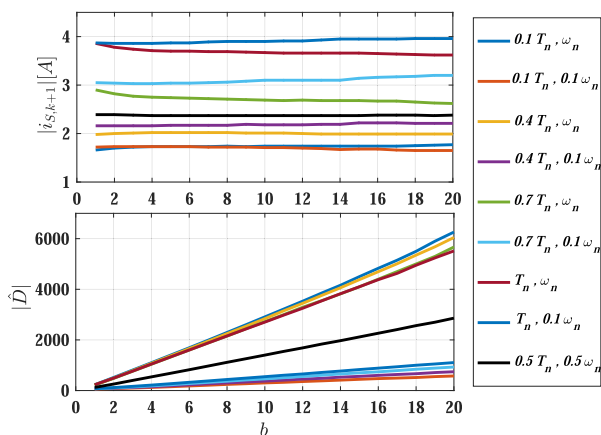


FIGURE 3. Effect of  $b$  on the predicted stator current and the estimated total disturbance in the different operating points.

The effect of the uncertainty for parameter  $b$  is studied in Fig. 3 for different operating points. It is seen that the stator current is robust against the change of the parameter  $b$  and the new total disturbance is successfully estimated. Thus, an initial rough estimation is enough for this parameter as below:

$$0.5 \frac{1}{\sigma L_s} < b < 1.5 \frac{1}{\sigma L_s} \quad (15)$$

### C. PARAMETER “ $\delta$ ”

This parameter is the boundary limit for the linear part of the  $f(e)$  function (8) to saturate the large feedbacks which are created by the measurement noise. For the linear area of  $f(e)$ ,

TDO turns to a typical linear observer with a pair of gains ( $\beta_1, \beta_2/\sqrt{\delta}$ ). The gains of a second-order linear observer are selected according to Hurwitz stability rule as follows:

$$s^2 + 2\beta_1 s + \beta_2/\sqrt{\delta} = (s + \omega_n)^2 \quad (16)$$

where  $\omega_n$  is natural frequency. It is deduced from (16) that  $\beta_1^2 = 4\beta_2/\sqrt{\delta}$ . So, by using the criterion that is proposed in (9), the acceptable range of  $\delta$  can be achieved as (17).

$$\frac{\beta_2}{(\sqrt{\delta})^2} > \beta_2 \rightarrow 0 < \delta < 1. \quad (17)$$

A practical way to select  $\delta$  is considering  $\delta = 1$  at first, which makes the TDO a linear observer, then by decreasing  $\delta$ , the optimum value for TDO can be found. In this research, it is set to  $\delta = 0.01$ .

## VI. SIMULATION RESULTS

The performance of the proposed control system and its robustness have been evaluated by the simulations in this section. The parameters of the tested motor are presented in Table 1. Note that the speed is 1350 r/min and the load torque is 5 N.m in all parameter sensitivity evaluations.

TABLE 1. Test system parameters.

Nominal rating of IM	
$P_n = 1.5$ kW	$R_s = 5$ $\Omega$
$V_n = 220$ V	$R_r = 4.9$ $\Omega$
$I_n = 3.9$ A	$L_s = 0.623$ H
$\omega_{r_m} = 1410$ r/min	$L_r = 0.623$ H
$f_s = 50$ Hz	$L_m = 0.591$ H
$T_n = 10.1$ N.m	$R_{fe} = 2403$ $\Omega$
$J = 0.065$ kg.m <sup>2</sup>	$P = 4$ poles
$t_s = 100$ $\mu$ s	$V_{dc} = 530$ V

### A. EVALUATION OF THE SENSITIVITY TO PARAMETER “b”

Fig. 4 shows the simulation results of the proposed control method for different values of the parameter “ $b$ ”. The parameter “ $b$ ” is set to the different proportions of  $b_0$ , where  $b_0 = 1/\sigma L_s$ . The results confirm the conclusion that was achieved by Fig. 3 and showed that the method is stable for all proportions of the  $b_0$ , and the accuracy is more for the boundary of  $\pm 50\%$ .

### B. EVALUATION OF THE SENSITIVITY TO PARAMETERS $\beta_1$ AND $\beta_2$

In order to analyze the effect of the parameters  $\beta_1$  and  $\beta_2$  on the performance of the proposed model, first  $M$  is approximately achieved from (12), which is  $M = 4.5 \times 10^5$ , and the values of  $\beta_1$  and  $\beta_2$  are chosen according to (13). Fig. 5 compares the simulation results for three different values of  $\beta_1$  and  $\beta_2$ . Note that  $\beta_{2o} = 6 \times 10^5$ , and  $\beta_1$  is relatively changed by (13). As it is evident, the proposed control method is stable for those cases because the selected values of  $\beta_1$  and  $\beta_2$  are satisfying the convergence criterion. However, very big values of feedback gains increase the ripples because the speed of the observer is decreased by

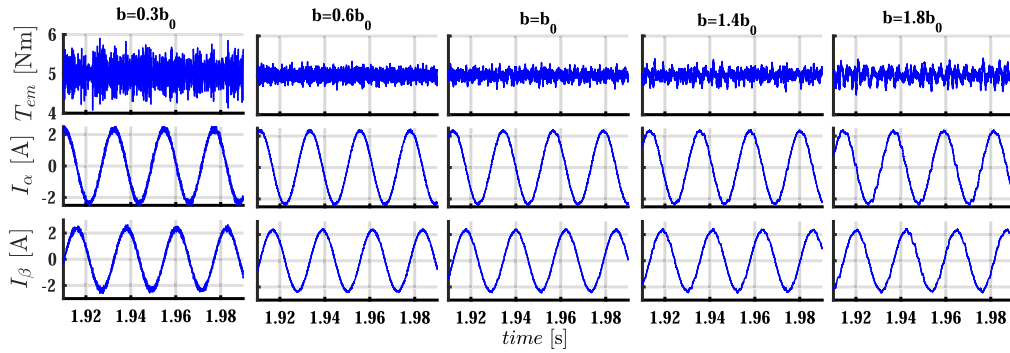


FIGURE 4. Effect of the variation of the parameter  $b$  on the IM performance.

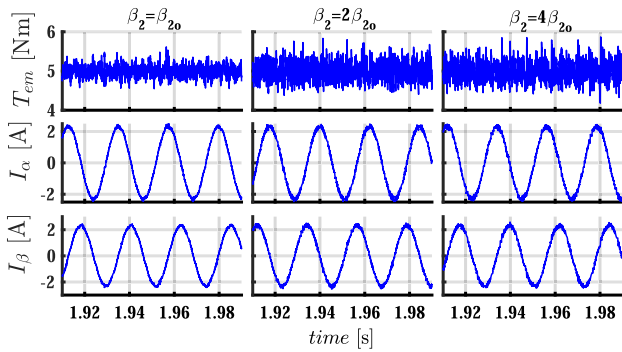


FIGURE 5. Simulation results when the parameter  $\beta_2$  is increasing.  $\beta_1$  is chosen according to each  $\beta_2$ .

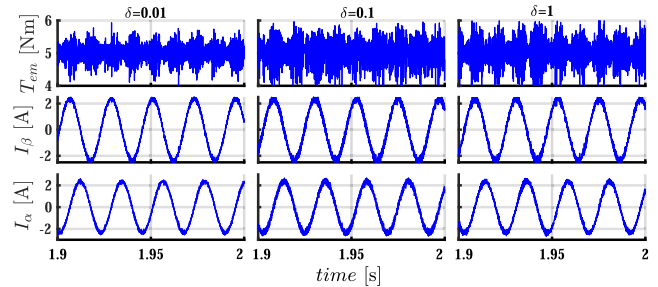


FIGURE 7. Studying the effect of parameter  $\delta$  when a white noise is added to the measured current.

simulation. The results are shown in Fig. 7 for three different values of  $\delta$ . The results confirm that the criterion  $0 < \delta < 1$  was correct and the best cancellation occurred in  $\delta = 0.01$ .

#### D. VARIATION OF THE STATOR AND ROTOR RESISTANCES

Results of the proposed control method and the classic PCC are compared while the stator and rotor resistances are gradually increasing. Fig. 8 compares the effect of the stator resistance variation, in which the results of classical PCC deteriorate when the stator resistance error reaches 40%. In contrast, the proposed FS-MPCC can tolerate the stator resistance error of up to 250%. Fig. 9 studies the rotor resistance variation. While the classical PCC has a distorted result for the errors of more than 30%, the proposed predictive model has a stable response until 150% error of the rotor resistance.

### VII. EXPERIMENTAL RESULTS

This section presents the experimental results of the proposed FS-MPCC. Fig. 10 shows the experimental set-up, and the parameters of the IM are the same as the simulation. The proposed method has been implemented by a DSP microprocessor TMS320F28335 with 150 MHz of maximum operating frequency, and the sampling time is set  $t_s = 100 \mu s$ .

#### A. OVERALL PERFORMANCE OF THE PROPOSED PCC

Fig. 11 shows the dynamic response of the proposed method in the no-load condition. The speed reference is set to the 50% synchronous speed, i.e., 750 r/min. The accurate and stable

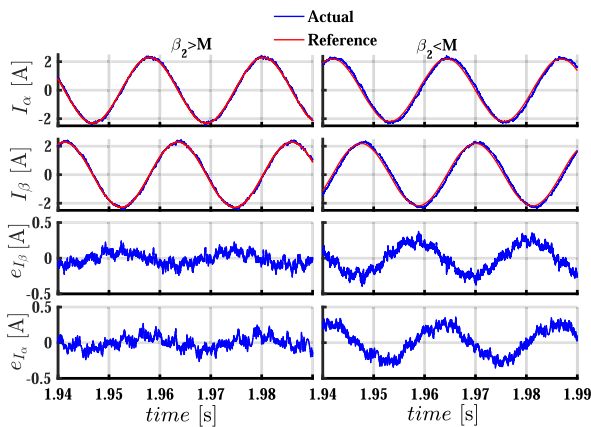
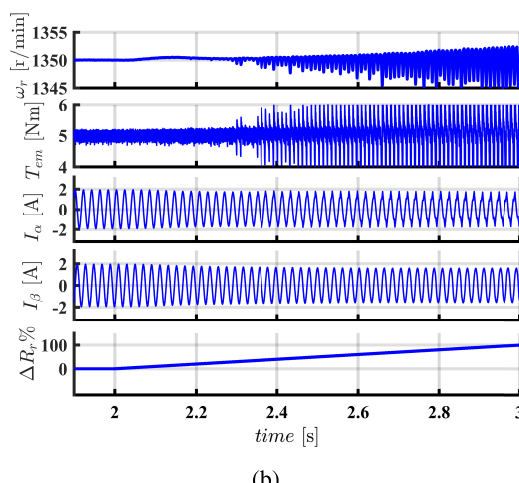
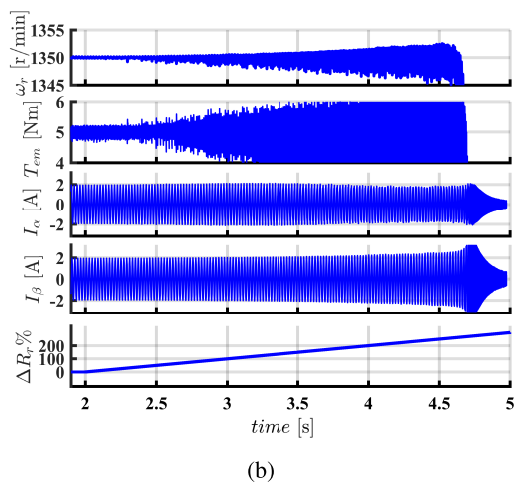
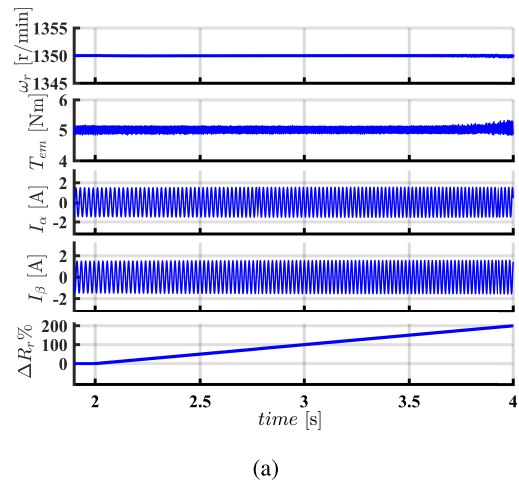
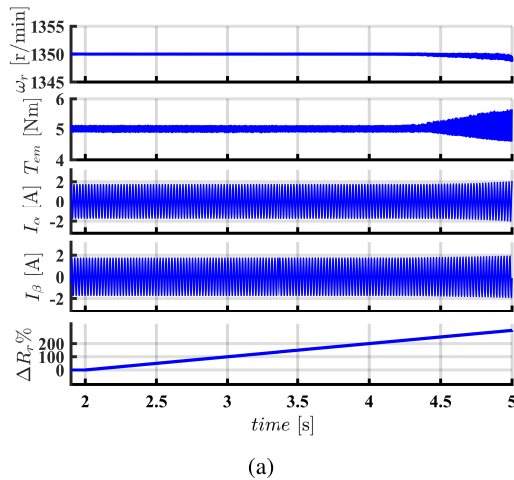


FIGURE 6. Effect of the convergence criterion of the proposed method on the stator current components.  $\beta_2 > M$  satisfies the criterion and  $\beta_2 < M$  does not satisfy it.

the raise of the gains. Also, Fig. 6 evaluates the effect of the convergence criterion (9). When  $\beta_2 = 2 \times 10^5$ , which does not satisfy the convergence criterion because  $\beta_2 < M$ , the stator current components do not track their references accurately. In contrast, when  $\beta_2 = 6 \times 10^5$  which means  $\beta_2 > M$ , the proposed control method showed a good tracking behavior.

#### C. EFFECT OF $\delta$ ON THE INPUT NOISES

To evaluate the effect of parameter  $\delta$  on the performance of the TDO, white noise is added to the input current in the



**FIGURE 8.** Effect of the stator resistance variation on the motor speed, electromagnetic torque,  $\alpha\beta$  components of stator current. (a) Proposed method (b) Classical PCC method.

**FIGURE 9.** Effect of the rotor resistance variation on the speed, electromagnetic torque,  $\alpha\beta$  components of the stator current. (a) Proposed method (b) Classical PCC method.

performance of the method can be concluded in the no-load condition. Note that since the proposed control system is based on the current control method, the stator flux has been automatically controlled on a relative value.

Fig. 12 presents the dynamic response of the proposed FS-MPCC when the IM is under a light mechanical load with a lower speed reference,  $\omega_r = 500$  r/min. This figure shows that the proposed model can keep the performance in a light load condition. Furthermore, Fig. 13 illustrates the behavior of the proposed control method where the speed reference is 1000 r/min and the load torque is 5 N.m. The average switching frequency is about 8 kHz, while the maximum switching frequency is set at 10 kHz. The results verify the effectiveness of the method in a wide operating condition.

**B. EVALUATION OF TDO**

To validate the proposed prediction model, the performance of TDO is experimentally studied. The sensitivity of the proposed PCC to parameter  $b$  is shown in Fig. 14. As mentioned in (15),  $b$  can be selected within the  $\pm 50\%$  range of the input coefficient. So, the performance of TDO is illustrated

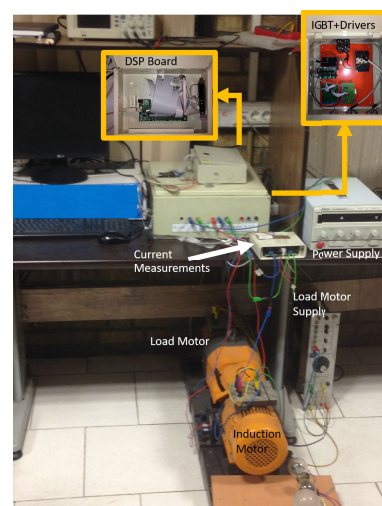


**FIGURE 10.** Experimental set-up.

for three different values:  $b = 10$ , which is the designed value,  $b = 14$ , and  $b = 6$ , i.e.,  $\pm 40\%$  of  $b$ . Even though the designed value  $b = 10$  has the best tracking response,

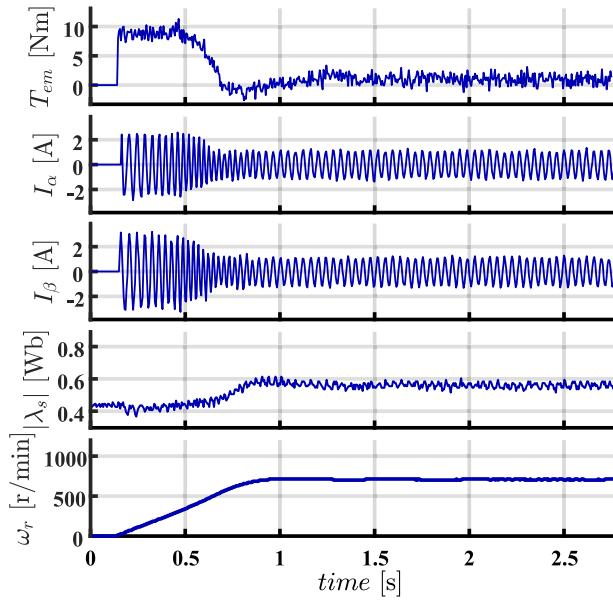


FIGURE 11. Performance of the proposed FS-MPCC method in no-load condition and 50% synchronous speed.

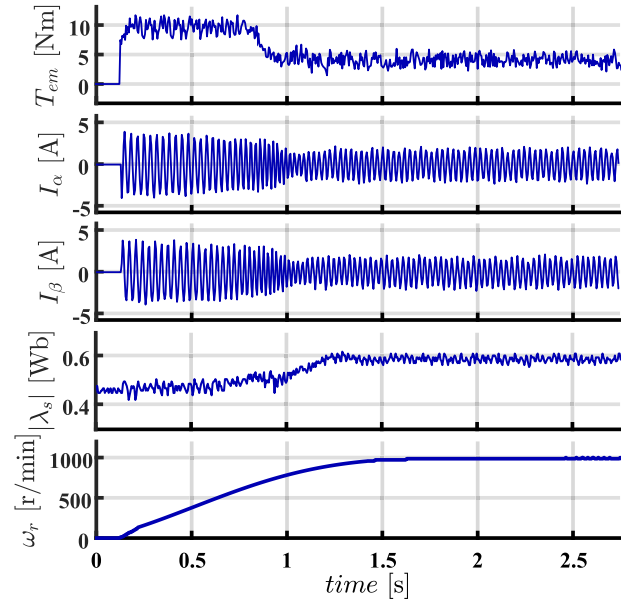


FIGURE 13. Performance of the proposed method when load torque is 5 Nm and the speed reference is 1000 r/min.

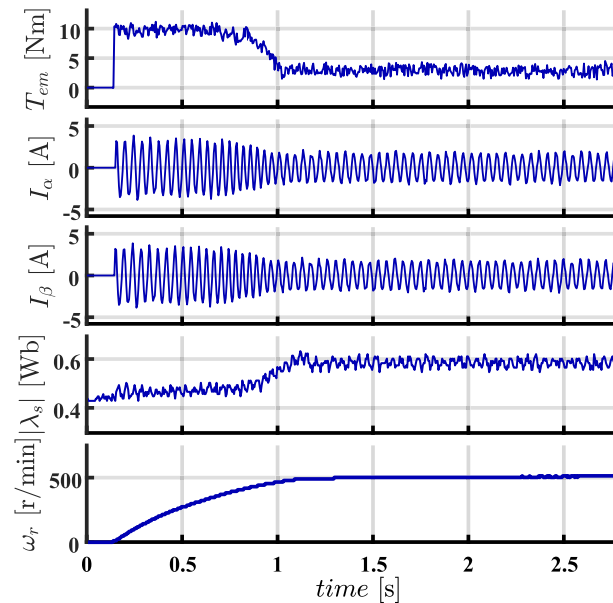


FIGURE 12. Performance of the proposed method under a light mechanical load when the speed reference is 500 r/min.

the error of TDO is less than 10% in the presence of 40% changes in  $b$ .

Fig. 15 shows the response of TDO for different values of  $\beta_1, \beta_2$ . Note that  $\beta_1$  is related to  $\beta_2$ . For the designed value of  $\beta_2$ , the output of TDO is shown in Fig. 15a. In this condition, the reference currents are precisely tracked by the current components. In Fig. 15b, the current ripples are increased by selecting a higher value for  $\beta_2$ . Also, in this condition, the reference currents are tracked by the outputs of TDO. When the convergence criterion (9) is violated in Fig. 15c, the currents are highly distorted, and the tracking errors are

TABLE 2. MSE for different tests of TDO.

Test	Fig.14a	Fig.14b	Fig.14c	Fig.15b	Fig.15c	Fig.16
RMSE of $I_\alpha$	2.5%	3.2%	3.7%	5%	8.1%	3.6%
RMSE of $I_\beta$	2.57%	3.5%	4.2%	6.2%	9.1%	3.8%
CoD for $I_\alpha$	0.994	0.99	0.987	0.982	0.943	0.982
CoD for $I_\beta$	0.994	0.988	0.983	0.98	0.932	0.981

increased. These results validate the proposed designing process for TDO.

The performance of the proposed TDO is evaluated in a dynamic condition where the stator current increases due to load change. Fig. 16 shows the dynamic response of TDO. In the transient condition, the current follows its reference value in a quarter of a cycle, which shows the fast-tracking response of TDO. To compare the test results in Fig. 14 to Fig. 16, the normalized root mean squared errors (RMSE) and the coefficient of determination (CoD) of estimations are calculated by (18) and (19), respectively. Note that the CoD is denoted by  $R^2$ . The results are presented in Table 2.

$$RMSE = \sqrt{\frac{\sum_{i=1}^n (i_s^* - \hat{i}_s)^2}{n}} \quad (18)$$

$$R^2 = 1 - \frac{\sum_{i=1}^n (\hat{i}_s^* - \hat{i}_s)^2}{\sum_{i=1}^n (i_s^* - \bar{i}_s)^2} \quad (19)$$

where  $n$  is the number of samples,  $i_s^*$  and  $\hat{i}_s$  are the reference and observed stator current, respectively. Also,  $\bar{i}_s$  is the mean of the measured samples of the stator current.

According to Table 2, TDO with the designed parameters has the lowest RMSE, and when the convergence criterion



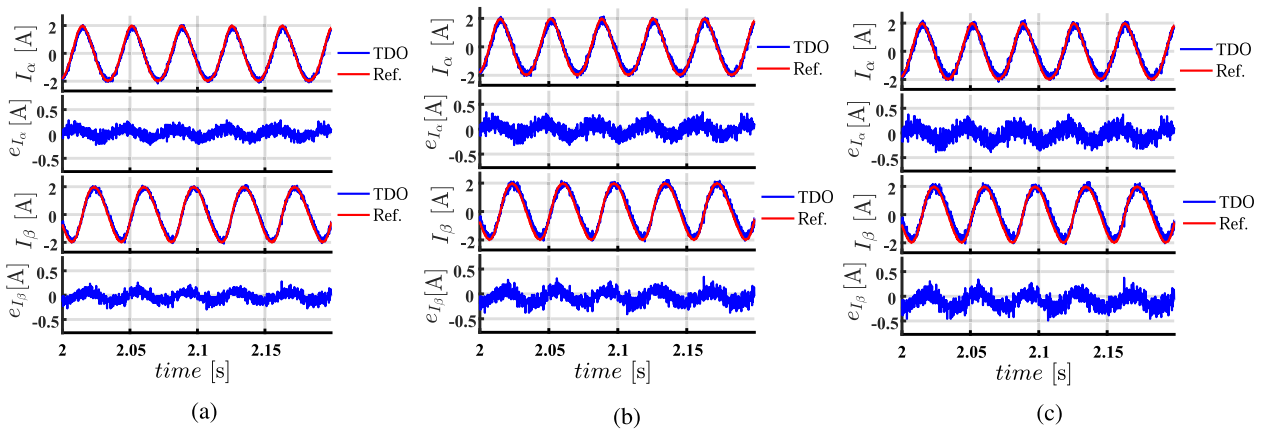


FIGURE 14. Experimental performance of TDO for different values of parameter  $b$  (a) designed value, (b) 40% increase for  $b$ , (c) 40% decrease for  $b$ .

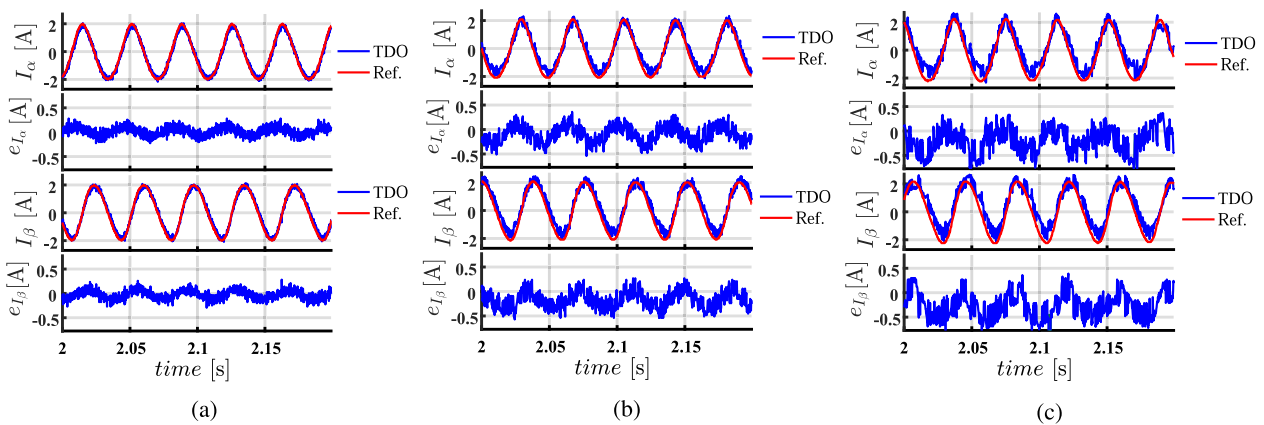


FIGURE 15. Experimental performance of TDO for different values of parameter  $\beta_2$  (a) designed value, (b) 100% increase for  $\beta_2$ , (c) when the convergence criterion is violated.

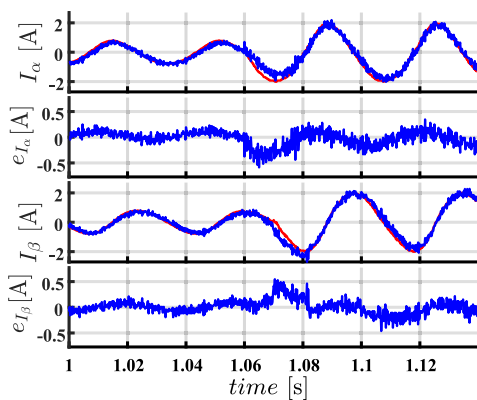
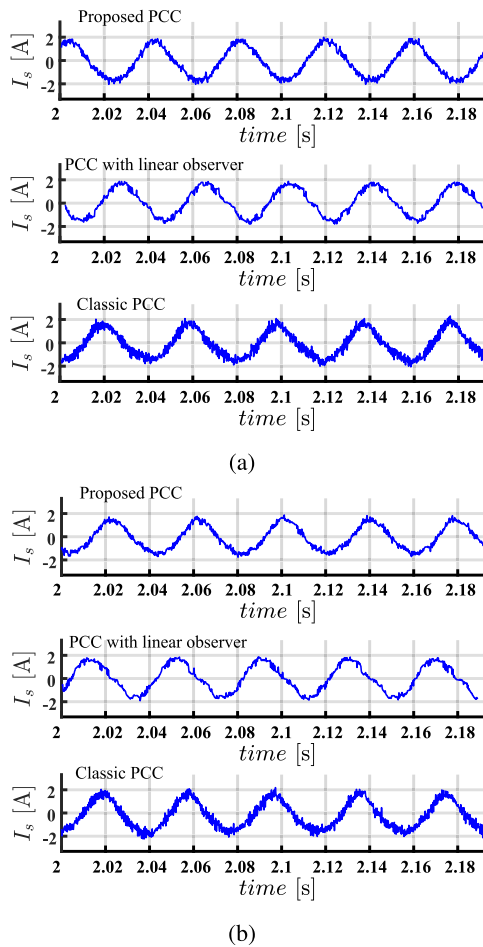


FIGURE 16. Dynamic response of TDO in the experiments.

is violated, the highest RMSE is obtained. Also, for the dynamic response in Fig. 16, RMSE is negligibly increased. For the TDO with the designed parameters,  $R^2$  is achieved near enough to 1. It means that the TDO almost has a perfect observation. On the contrary,  $R^2$  is decreased when the convergence criterion is violated.

### C. COMPARISON OF THE PROPOSED METHOD WITH OTHER MPC METHODS

To effectively show the performance of the proposed control method, it is compared with two different robust MPC schemes in the literature. One is an MRAS-based robust FS-MPC [11], and the other is a linear disturbance observer-based PCC [15]. The current prediction model of these methods has been implemented in the experimental tests, and their results are compared with the proposed method results. These three control systems have been tested within a normal condition, and their steady-state results are shown in Fig. 17a. Also, the robustness of these methods is compared in Fig. 17b when a  $4.7 \Omega$  physical resistance is connected in series with each of the stator windings. While the methods are robust against the variation of the stator resistance, the response of the proposed method showed lower current distortion. The quantified results are summarized in Table 3. It can be seen the proposed PCC method has a lower current THD. It must be noted that the proposed control method has a more robust response against the variation of the stator resistance. Because by increasing the stator resistance,



**FIGURE 17.** Experimental results for the proposed method, linear observer-based PCC in [15], and method in [11]: steady-state stator current for (a) normal condition (b) the stator resistance increases by 94%.

**TABLE 3.** Comparison of the current THD.

Test condition	Execution Time ( $\mu s$ )	Normal Condition	When $\Delta R_s = 94\%$
Model in [11]	43	17.5%	22.4%
Model in [15]	34	14.3%	17.8%
Proposed model	36	9.8%	11.4%

the variation of THD for the proposed method is less than the other methods. Furthermore, the execution time of each method is given in Table 3.

### VIII. CONCLUSION

A robust current prediction model was proposed in this paper for the FS-MPCC scheme. The principle of the ADRC strategy was used in a feed-forward formation to achieve compatibility with the FS-MPCC technique. Opposite to the classic disturbance rejection techniques, the disturbance observer is the main part of the prediction model. In this model, all of the system disturbances and model uncertainties were lumped into a single variable which was estimated by TDO. A thorough guideline was proposed for tuning the local parameters of the observer, which are less than the

classic disturbance rejection based predictive methods. The convergence analysis of TDO was studied in this paper by using the self-stable region approach and Lyapunov theory. The results of the simulations and experiments verified the accuracy and the robustness of the proposed control system. The THD of the current is improved compared to the robust MRAS-based FS-MPC.

### APPENDIX CONVERGENCE ANALYSIS OF TDO

The error system of the TDO can be attained from (7) by considering  $e_1 = i_s - \hat{i}_s$ ,  $e_2 = D - \hat{D}$  as follows

$$\dot{e}_1 = e_2 - \beta_1 e_1 \tag{20a}$$

$$\dot{e}_2 = G(t) - \beta_2 \times f(e_1) \tag{20b}$$

where  $G(t)$  is the time derivative of  $D$ . A convergence study tool is proposed in [30] for such uncertain models which is called “self-stable region” (SSR) approach.

The defined region  $z(e_1, e_2)$  is an SSR for the error system (20) with the following definition

$$z(e_1, e_2) = \{(e_1, e_2) : |h(e_1, e_2)| \leq g(e_1)\} \tag{21a}$$

$$h(e_1, e_2) = e_2 - \beta_1 e_1 + (\beta_2/\beta_1)f(e_1) \tag{21b}$$

$$g(e_1) = \beta_2/(k\beta_1)|f(e_1)| \tag{21c}$$

where  $k > 1$  is a constant.

It should be proved that all of the trajectories  $(e_1, e_2)$  inside the region will converge to the origin  $(0, 0)$ . To fulfill this purpose a Lyapunov candidate function is defined as

$$V_1 = \frac{1}{2}g^2(e_1) \tag{22}$$

The error system (20) is convergent when the condition  $\dot{V}_1 < 0$  is correct. Since  $|h(e_1, e_2)| \leq g(e_1)$ , the  $|h(e_1, e_2)|$  will be stable if  $g(e_1)$  is stable.

$$\begin{aligned} \dot{V}_1 &= g(e_1)\dot{g}(e_1) = (\beta_2/(k\beta_1))^2 f(e_1) \frac{\partial f(e_1)}{\partial e_1} \dot{e}_1 \\ &= \left(\frac{\beta_2}{k\beta_1}\right)^2 f(e_1) \frac{\partial f(e_1)}{\partial e_1} (e_2 - \beta_1 e_1) \end{aligned} \tag{23}$$

In (23),  $(\beta_2/k\beta_1)^2$  is always positive and  $f(e_1)$  is a monotonically increasing function, i.e.,  $\partial f(e_1)/\partial e_1 > 0$ . Therefore, it is important to prove  $f(e_1)(e_2 - \beta_1 e_1) < 0$ .

To do so, both sides of (21a) are multiplied by  $f(e_1)$  and the following is derived:

$$f(e_1)(e_2 - \beta_1 e_1) < \frac{\beta_2(1-k)}{k\beta_1} f^2(e_1). \tag{24}$$

It is clear that for  $k > 1$  and positive gains  $\beta_1, \beta_2$  the right side of (24) is negative and consequently based on (23) the condition  $\dot{V}_1 < 0$  is always true.

Now, a criterion should be found that guarantees the trajectories outside of the region  $z$ , i.e.,  $|h(e_1, e_2)| > g(e_1)$  will be converged inside. The Lyapunov function for those trajectories is expressed as

$$V_1 = \frac{1}{2}(h^2(e_1, e_2) - g^2(e_1)). \tag{25}$$

The derivative of the Lyapunov candidate by considering  $\dot{e}_2 - \beta_1 \dot{e}_1 = G - \beta_1 h$  based on (20), and  $\dot{e}_1 = e_2 - \beta_1 e_1 = h - f\beta_2/\beta_1$  based on (20-a) and (21-b), is as follows,

$$\dot{V}_1 = Gh - \beta_1 h^2 + \frac{\beta_2}{\beta_1} \frac{\partial f}{\partial e_1} (h - \frac{\beta_2 f}{\beta_1}) (h - \frac{\beta_2}{k^2 \beta_1} f). \quad (26)$$

where  $h = h(e_1, e_2)$ ,  $G = G(t)$ , and  $f = f(e_1)$ .

On the other hand, by using

$$(h - \frac{\beta_2 f}{\beta_1}) (h - \frac{\beta_2}{k^2 \beta_1} f) = h^2 + (\frac{\beta_2 f}{\beta_1 k})^2 - \frac{\beta_2}{\beta_1} f h (1 + \frac{1}{k^2}) \quad (27)$$

and considering  $g = \beta_2 |f| / (k\beta_1) < h$ , and  $1 + 1/k^2 < 2$ , the following inequality is acceptable:

$$h^2 + (\frac{\beta_2 f}{\beta_1 k})^2 - \frac{\beta_2}{\beta_1} f h (1 + \frac{1}{k^2}) < h^2 + g^2 + gh(1 + \frac{1}{k^2}) < 4h^2. \quad (28)$$

Now with using (28), if  $m < 1$  is considered as an arbitrary constant and  $m\beta_1 h^2$  is added and subtracted by (26), the condition  $\dot{V}_1 < 0$  can be achieved with two constraints:

$$-m\beta_1 + 4 \frac{\beta_2}{\beta_1} \frac{\partial f(e_1)}{\partial e_1} \leq 0 \Rightarrow \beta_1^2 \geq 4 \frac{\beta_2}{m} \frac{\partial f(e_1)}{\partial e_1} \quad (29a)$$

$$Mh - (1 - m)\beta_1 h^2 < 0 \Rightarrow \beta_1 h > \frac{M}{1 - m}. \quad (29b)$$

From (29a) the left side of (9) can be deduced.

On the other hand,  $\beta_1 h > \beta_2 |f| / k$  is concluded again based on  $g = \beta_2 |f| / (k\beta_1) < h$ . Thus, considering  $k > 1$  and  $(1 - m) > 1$ , if the following condition is fulfilled so will the criterion of (29b).

$$\beta_2 |f| > M \quad (30)$$

## REFERENCES

- [1] P. Karamanakos, E. Liegmann, T. Geyer, and R. Kennel, "Model predictive control of power electronic systems: Methods, results, and challenges," *IEEE Open J. Ind. Appl.*, vol. 1, pp. 95–114, 2020.
- [2] J. Rodríguez, M. P. Kazmierkowski, J. R. Espinoza, P. Zanchetta, H. Abu-Rub, H. A. Young, and C. A. Rojas, "State of the art of finite control set model predictive control in power electronics," *IEEE Trans. Ind. Informat.*, vol. 9, no. 2, pp. 1003–1016, May 2013.
- [3] S. A. Davari, F. Wang, and R. M. Kennel, "Robust deadbeat control of an induction motor by stable MRAS speed and stator estimation," *IEEE Trans. Ind. Informat.*, vol. 14, no. 1, pp. 200–209, Jan. 2018.
- [4] Y. Zhang, H. Yang, and B. Xia, "Model-predictive control of induction motor drives: Torque control versus flux control," *IEEE Trans. Ind. Appl.*, vol. 52, no. 5, pp. 4050–4060, Sep./Oct. 2016.
- [5] X.-H. Jin, Y. Zhang, and D.-G. Xu, "Static current error elimination algorithm for induction motor predictive current control," *IEEE Access*, vol. 5, pp. 15250–15259, 2017.
- [6] J. Wang, F. Wang, G. Wang, S. Li, and L. Yu, "Generalized proportional integral observer based robust finite control set predictive current control for induction motor systems with time-varying disturbances," *IEEE Trans. Ind. Informat.*, vol. 14, no. 9, pp. 4159–4168, Sep. 2018.
- [7] M. Siami, D. A. Khaburi, and J. Rodríguez, "Torque ripple reduction of predictive torque control for PMSM drives with parameter mismatch," *IEEE Trans. Power Electron.*, vol. 32, no. 9, pp. 7160–7168, Sep. 2017.
- [8] M. Yang, X. Lang, J. Long, and D. Xu, "Flux immunity robust predictive current control with incremental model and extended state observer for PMSM drive," *IEEE Trans. Power Electron.*, vol. 32, no. 12, pp. 9267–9279, Dec. 2017.
- [9] J. Wang, F. Wang, Z. Zhang, S. Li, and J. Rodriguez, "Design and implementation of disturbance compensation-based enhanced robust finite control set predictive torque control for induction motor systems," *IEEE Trans. Ind. Informat.*, vol. 13, no. 5, pp. 2645–2656, Oct. 2017.
- [10] Y. B. Zbiede, S. M. Gadoue, and D. J. Atkinson, "Model predictive MRAS estimator for sensorless induction motor drives," *IEEE Trans. Ind. Electron.*, vol. 63, no. 6, pp. 3511–3521, Jun. 2016.
- [11] A. Aliaskari, B. Zarei, S. A. Davari, F. Wang, and R. M. Kennel, "A modified closed-loop voltage model observer based on adaptive direct flux magnitude estimation in sensorless predictive direct voltage control of an induction motor," *IEEE Trans. Power Electron.*, vol. 35, no. 1, pp. 630–639, Jan. 2020.
- [12] M. Ouhrouche, R. Errouissi, A. M. Trzynadlowski, K. Tehrani, and A. Benzaïoua, "A novel predictive direct torque controller for induction motor drives," *IEEE Trans. Ind. Electron.*, vol. 63, no. 8, pp. 5221–5230, Aug. 2016.
- [13] C. Fu and W. Tan, "Linear active disturbance rejection control for processes with time delays: IMC interpretation," *IEEE Access*, vol. 8, pp. 16606–16617, 2020.
- [14] L. Yan, F. Wang, M. Dou, Z. Zhang, R. Kennel, and J. Rodriguez, "Active disturbance-rejection-based speed control in model predictive control for induction machines," *IEEE Trans. Ind. Electron.*, vol. 67, no. 4, pp. 2574–2584, Apr. 2020.
- [15] Y. Zhang, J. Jin, and L. Huang, "Model-free predictive current control of PMSM drives based on extended state observer using ultralocal model," *IEEE Trans. Ind. Electron.*, vol. 68, no. 2, pp. 993–1003, Feb. 2021.
- [16] Y. Wang, H. Li, R. Liu, L. Yang, and X. Wang, "Modulated model-free predictive control with minimum switching losses for PMSM drive system," *IEEE Access*, vol. 8, pp. 20942–20953, 2020.
- [17] F. Tinazzi, P. G. Carlet, S. Bolognani, and M. Zigliotto, "Motor parameter-free predictive current control of synchronous motors by recursive least-square self-commissioning model," *IEEE Trans. Ind. Electron.*, vol. 67, no. 11, pp. 9093–9100, Nov. 2020.
- [18] A. Brosch, S. Hanke, O. Wallscheid, and J. Bocker, "Data-driven recursive least squares estimation for model predictive current control of permanent magnet synchronous motors," *IEEE Trans. Power Electron.*, vol. 36, no. 2, pp. 2179–2190, Feb. 2021.
- [19] J. Han, "From PID to active disturbance rejection control," *IEEE Trans. Ind. Electron.*, vol. 56, no. 3, pp. 900–906, Mar. 2009.
- [20] Y. Huang and W. Xue, "Active disturbance rejection control: Methodology and theoretical analysis," *ISA Trans.*, vol. 53, no. 4, pp. 963–976, 2014.
- [21] G. Feng, Y.-F. Liu, and L.-P. Huang, "A new robust algorithm to improve the dynamic performance on the speed control of induction motor drive," *IEEE Trans. Power Electron.*, vol. 19, no. 6, pp. 1614–1627, Nov. 2004.
- [22] J. Li, H.-P. Ren, and Y.-R. Zhong, "Robust speed control of induction motor drives using first-order auto-disturbance rejection controllers," *IEEE Trans. Ind. Appl.*, vol. 51, no. 1, pp. 712–720, Jan. 2015.
- [23] F. Alonge, M. Cirrincione, F. D'Ippolito, M. Pucci, and A. Sferlazza, "Robust active disturbance rejection control of induction motor systems based on additional sliding-mode component," *IEEE Trans. Ind. Electron.*, vol. 64, no. 7, pp. 5608–5621, Jul. 2017.
- [24] M. Fliess and C. Join, "Model-free control," *Int. J. Control*, vol. 86, no. 12, pp. 2228–2252, 2013.
- [25] O. Wallscheid and E. F. B. Ngoumtsa, "Investigation of disturbance observers for model predictive current control in electric drives," *IEEE Trans. Power Electron.*, vol. 35, no. 12, pp. 13563–13572, Dec. 2020.
- [26] T. Geyer, "Algebraic tuning guidelines for model predictive torque and flux control," *IEEE Trans. Ind. Appl.*, vol. 54, no. 5, pp. 4464–4475, Sep. 2018.
- [27] R. Yang, M.-Y. Wang, L.-Y. Li, C.-M. Zhang, and J.-L. Jiang, "Robust predictive current control with variable-gain adaptive disturbance observer for PMLSM," *IEEE Access*, vol. 6, pp. 13158–13169, 2018.
- [28] C. Xu, Z. Han, and S. Lu, "Deadbeat predictive current control for permanent magnet synchronous machines with closed-form error compensation," *IEEE Trans. Power Electron.*, vol. 35, no. 5, pp. 5018–5030, May 2020.
- [29] V. Utkin, J. Guldner, and M. Shijun, *Sliding Mode Control Electro-Mechanical System*, vol. 34. Boca Raton, FL, USA: CRC Press, 1999.
- [30] Y. Huang and J. Han, "Analysis and design for the second order nonlinear continuous extended states observer," *Chin. Sci. Bull.*, vol. 45, no. 21, p. 1938, 2000.



**MAHDI S. MOUSAVI** received the B.Sc. and M.Sc. degrees in electrical engineering from Iran University of Science and Technology (IUST), Tehran, Iran, in 2013 and 2015, respectively. He is currently pursuing the Ph.D. degree with Shahid Rajaei Teacher Training University (SRTTU), Tehran. His current research interests include variable-speed drives and model predictive control.



**S. ALIREZA DAVARI** (Senior Member, IEEE) was born in Tehran, Iran, in 1981. He received the M.Sc. and Ph.D. degrees from Iran University of Science and Technology (IUST), Tehran, in 2006 and 2012, respectively. Between 2010 and 2011, he left for a sabbatical visit at Technische Universität München, Germany. Since 2013, he has been an Assistant Professor with Shahid Rajaei Teacher Training University. His research interests include encoder-less drives, predictive control, power electronics, and renewable energy.



**VAHAB NEKOUKAR** received the B.Sc. degree in electrical engineering from Khaje Nasir Toosi University, in 2005, the M.Sc. degree in electrical engineering from Tarbiat Modares University, in 2007, and the Ph.D. degree in electrical engineering from Iran University of Science and Technology, in 2012. In 2014, he joined the School of Electrical Engineering, Shahid Rajaei Teacher Training University, as an Assistant Professor. His current research interests include control of biological systems, robotics, navigation, and guidance systems.



**CRISTIAN GARCIA** (Member, IEEE) received the M.Sc. and Ph.D. degrees in electronics engineering from Universidad Tecnica Federico Santa Maria (UTFSM), Valparaiso, Chile, in 2013 and 2017, respectively. In 2016, he was a visiting Ph.D. student in the Power Electronics Machines and Control (PEMC) Group, University of Nottingham, U.K. From 2017 to 2019, he was with the Engineering Faculty, Universidad Andres Bello, Santiago, Chile, as an Assistant Professor.

Since 2019, he has been with the Department of Electrical Engineering, University of Talca, Curico, Chile, where he is currently an Assistant Professor. His research interests include electric transportation applications, variable-speed drives, and model predictive control of power converters and drives.



**JOSE RODRIGUEZ** (Life Fellow, IEEE) received the degree in electrical engineering from Universidad Tecnica Federico Santa Maria, Valparaiso, Chile, in 1977, and the Dr.-Ing. degree in electrical engineering from the University of Erlangen-Nürnberg, Erlangen, Germany, in 1985. He has been with the Department of Electronics Engineering, Universidad Tecnica Federico Santa Maria, since 1977, where he was a Full Professor and the President. Since 2015, he was the President

and has been a Full Professor at Universidad Andres Bello, Santiago, Chile, since 2019. He has coauthored two books, several book chapters, and more than 400 journals and conference papers. His research interests include multilevel inverters, new converter topologies, control of power converters, and adjustable-speed drives. He has received a number of best paper awards from journals of the IEEE. He is a member of the Chilean Academy of Engineering. In 2014, he received the National Award of Applied Sciences and Technology from the Government of Chile and the Eugene Mittelmann Award from the Industrial Electronics Society of the IEEE, in 2015. From 2014 to 2019, he has been included in the list of highly cited researchers published by Web of Science.

...